

## Open heavy flavour measurements in $p$ Pb collisions at LHCb

---

**Patrick Robbe**<sup>\*†</sup>

*LAL, Université Paris-Sud, CNRS/IN2P3, Orsay, France*

*E-mail: [robbe@lal.in2p3.fr](mailto:robbe@lal.in2p3.fr)*

Production of heavy flavour quarks in proton-lead collisions is a powerful tool to understand the properties of matter in heavy ion collisions and to characterize cold nuclear matter effects. New results from the LHCb experiment on the measurement of the cross-section of open charm mesons in  $p$ Pb collisions at the LHC at 5 TeV centre-of-mass energy are presented.

*The European Physical Society Conference on High Energy Physics  
5-12 July, 2017  
Venice*

---

<sup>\*</sup>Speaker.

<sup>†</sup>For the LHCb collaboration

## 1. Introduction

Measurements of charm quark production provide important information about the mechanisms occurring in the medium formed in proton-lead collisions [1]. These processes, called also "Cold Nuclear Matter" (CNM) effects, are competing with effects due to the screening of the strong interaction and de-confinement in high energy heavy ion collisions, such as suppression of charmonium production observed at the SPS [2], RICH [3] or LHC [4][5]. They must be precisely known in order to disentangle them. In addition, measurements of open charm production can help investigating the charm probability density in the partons. A new measurement of the prompt  $D^0$  production in  $pPb$  and  $Pb p$  collisions at 5 TeV was obtained analysing the LHCb data recorded during the 2013 LHC proton-lead run [6] and is presented here.

## 2. The LHCb experiment and its heavy ion program

The LHCb detector is described in details in Ref. [7][8]. It is optimized for the study of  $b$  and  $c$  hadrons produced in low pile-up  $pp$  collisions at the LHC. However the excellent performances reached in higher multiplicity proton-lead collisions are perfect for the measurement of heavy flavour in this environment. The detector covers the forward region with respect to the collision point,  $2 < \eta < 5$ , where  $\eta$  is the pseudo-rapidity of the detected particles. When the energies of the beams are asymmetric, which is the case at the LHC for proton-lead collisions, the acceptance in centre-of-mass rapidity,  $y^*$ , is  $1.5 < y^* < 4.0$  when the proton beam direction is pointing towards LHCb (called  $pPb$  configuration), and  $-5.0 < y^* < -2.5$  when the beams are reversed ( $Pb p$  configuration). This allows the experiment to record data in two different configurations and to probe different regions of  $x$ , the fractions of the longitudinal momentum carried by the colliding partons.

The most important features of the detector for measurements of heavy flavour production are: track reconstruction down to very low momentum to reconstruct hadrons down to zero transverse momentum ( $p_T$ ) where nuclear effects are expected to be the largest; precise decay vertex reconstruction to be able to separate hadrons produced directly at the collision point (*prompt* production) from those coming from the decay of a  $b$  hadron; particle identification based on RICH detectors to reconstruct decays in purely hadronic final states.

The experiment started collecting heavy ion data in 2013 during the LHC proton-lead run at a center-of-mass energy of 5 TeV. A total integrated luminosity of  $1.6 \text{ nb}^{-1}$  was recorded,  $1.1 \text{ nb}^{-1}$  in the  $pPb$  configuration and  $0.5 \text{ nb}^{-1}$  in the  $Pb p$  configuration. In 2015, the experiment took part to the  $PbPb$  run and collected  $50 \times 10^6$  minimum bias events at 5.02 TeV center-of-mass energy, and at the end of 2016,  $28 \text{ nb}^{-1}$  of proton-lead collisions ( $12 \text{ nb}^{-1}$  of  $pPb$  and  $16 \text{ nb}^{-1}$  of  $Pb p$ ) were recorded at a center-of-mass energy of 8.16 TeV. In addition, the experiment is developing a fixed target program and acquired collisions of protons or lead ions of the LHC beam with a gaseous fixed target injected at the interaction point with the so-called SMOG system (System to Measure Overlap with Gas, originally designed to measure the luminosity at LHCb). Various gases were used already as target (Ne, Ar, He) and first measurements obtained recently [9][10].

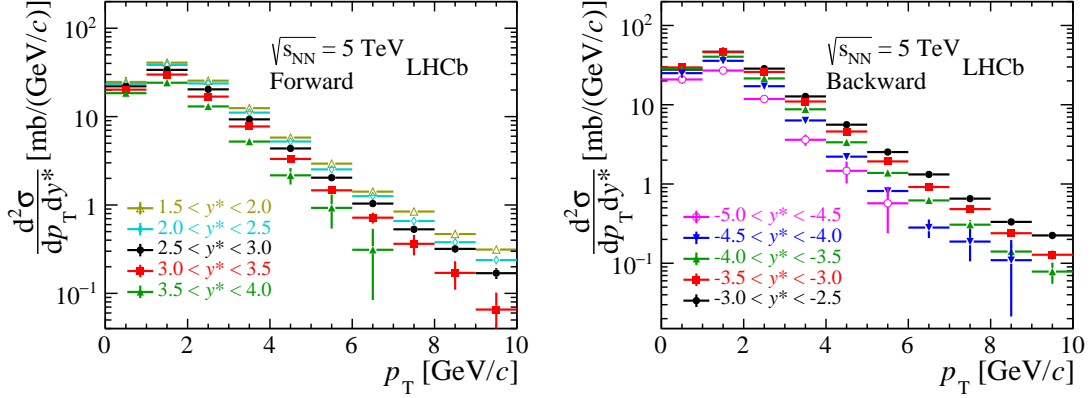


**Figure 1:** Prompt  $D^0$  production cross-sections, as a function of  $p_T$  and  $y^*$  for  $p\text{Pb}$  (left) and  $\text{Pb}p$  (right).

### 3. Prompt $D^0$ production in $p\text{Pb}$ collisions

For this measurement,  $D^0$  (and  $\bar{D}^0$ ) candidates are reconstructed in the decay mode  $D^0 \rightarrow K^- \pi^+$ , using tight particle identification criteria based on the RICH detectors. Only prompt  $D^0$  are considered, the  $D^0$  coming from  $b$  hadron decays are rejected based on their impact parameter with respect to the collision vertex. The double-differential absolute production cross-sections,  $\frac{d^2\sigma}{dp_T dy^*}$ , are obtained in bins of  $p_T$  and  $y^*$  of the meson, in the ranges  $0 < p_T < 10 \text{ GeV}/c$  and  $1.5 < y^* < 4.0$  (for  $p\text{Pb}$ ) or  $-5.0 < y^* < -2.5$  (for  $\text{Pb}p$ ). The numbers of signal candidates are extracted from a fit to their invariant mass distributions and are corrected by the total detection and reconstruction efficiencies computed from detailed Monte Carlo simulation. These efficiencies are corrected to take into account effects due to detector occupancy. The integrated luminosity of the sample used is determined from a van der Meer scan and beam gas imaging techniques detailed in Ref. [11]. The results are shown in Fig. 1 both for  $p\text{Pb}$  (left) and  $\text{Pb}p$  (right). The uncertainties on the measurements include both statistical and systematic uncertainties. The latter vary between 5% and 20% and are dominated by particle identification efficiency uncertainties.

The total cross-sections, integrated over the full analysis range, are measured equal to

$$\sigma_{p\text{Pb}}(p_T < 10 \text{ GeV}/c, 1.5 < y^* < 4.0) = 230.6 \pm 0.5 \pm 13.0 \text{ mb}, \quad (3.1)$$

$$\sigma_{\text{Pb}p}(p_T < 10 \text{ GeV}/c, -5.0 < y^* < -2.5) = 252.7 \pm 1.0 \pm 20.0 \text{ mb}, \quad (3.2)$$

where the first uncertainty is statistical and the second is systematic. Figure 2 shows the single-differential cross-sections as a function of  $p_T$  (left) and  $y^*$  (right) respectively, integrated over the other variable. On these two figures, a comparison with the HELAC-Onia tool [12] is shown. This generator is tuned to reproduce measurements performed in  $pp$  collisions and is used with different nuclear parton distribution functions (nPDF): EPS09LO, EPS09NLO [13] and nCTEQ15 [14].

### 4. Cold nuclear matter effects in $D^0$ production

CNM effects are studied comparing the production cross-sections in proton-lead collisions with the ones in proton-proton collisions at the same energy. The measurement of the prompt

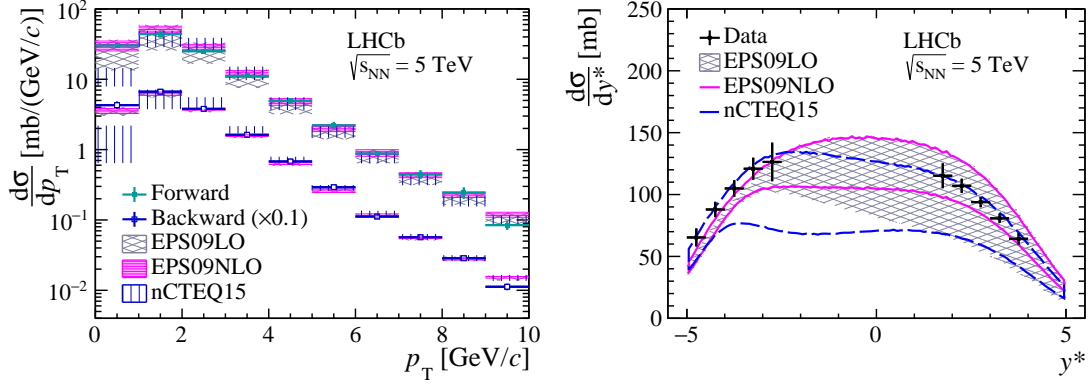


**Figure 2:** Prompt  $D^0$  production cross-sections, as a function of  $p_T$  (left, integrated over  $y^*$ ) and  $y^*$  (right, integrated over  $p_T$ ), for  $pPb$  and  $Pb p$ .

$D^0$  reference cross-section in  $pp$  at 5 TeV was performed using the data collected in 2015 [15] when  $8.6 \text{ pb}^{-1}$  of  $pp$  collisions were recorded during a dedicated LHC run at this energy. From these cross-sections and the ones presented in Sec. 3, the nuclear modification factor  $R_{pPb}$  and the forward-backward ratio  $R_{FB}$  are extracted, as a function of  $p_T$  and  $y^*$ . These quantities are defined as

$$R_{pPb}(p_T, y^*) = \frac{1}{A} \frac{d^2 \sigma_{pPb}(p_T, y^*) / dp_T dy^*}{d^2 \sigma_{pp}(p_T, y^*) / dp_T dy^*} \quad (4.1)$$

$$R_{FB}(p_T, y^*) = \frac{d^2 \sigma_{pPb}(p_T, +|y^*|) / dp_T dy^*}{d^2 \sigma_{Pb p}(p_T, -|y^*|) / dp_T dy^*}, \quad (4.2)$$

with  $A = 208$ . They should be equal to unity in the absence of CNM.

Figures 3 and 4 show the results as a function of  $p_T$  and  $y^*$  for  $R_{pPb}$  and  $R_{FB}$  respectively. On these figures are superimposed theoretical predictions using various models for the description of CNM. HELAC-Onia is used to illustrate the shadowing and anti-shadowing effects due to the modification of the gluon density functions inside the lead nucleons compared to protons, parametrized with various nPDFs sets (EPS09LO, EPS09NLO and nCTEQ15). The Color Glass Condensate model computations [16] are also compared with the experimental measurements. On these plots, a significant suppression of  $D^0$  production in proton-lead collisions compared to  $pp$  collisions can be observed, at low  $p_T$  in the forward region (positive rapidities). This effect is reproduced by the theoretical models within large uncertainties.

## 5. Conclusions and prospects

A precise measurement of the suppression of prompt  $D^0$  production was obtained analysing the proton-lead collisions recorded at LHCb in 2013. These results show a large suppression at forward rapidities and low transverse momentum, sign of Cold Nuclear Matter effects in these collisions. Other measurements of open heavy flavour production by LHCb will be possible in the near future, such as  $\Lambda_c^+$  production at 5 TeV. Several  $b$ -hadron species could also be reconstructed in

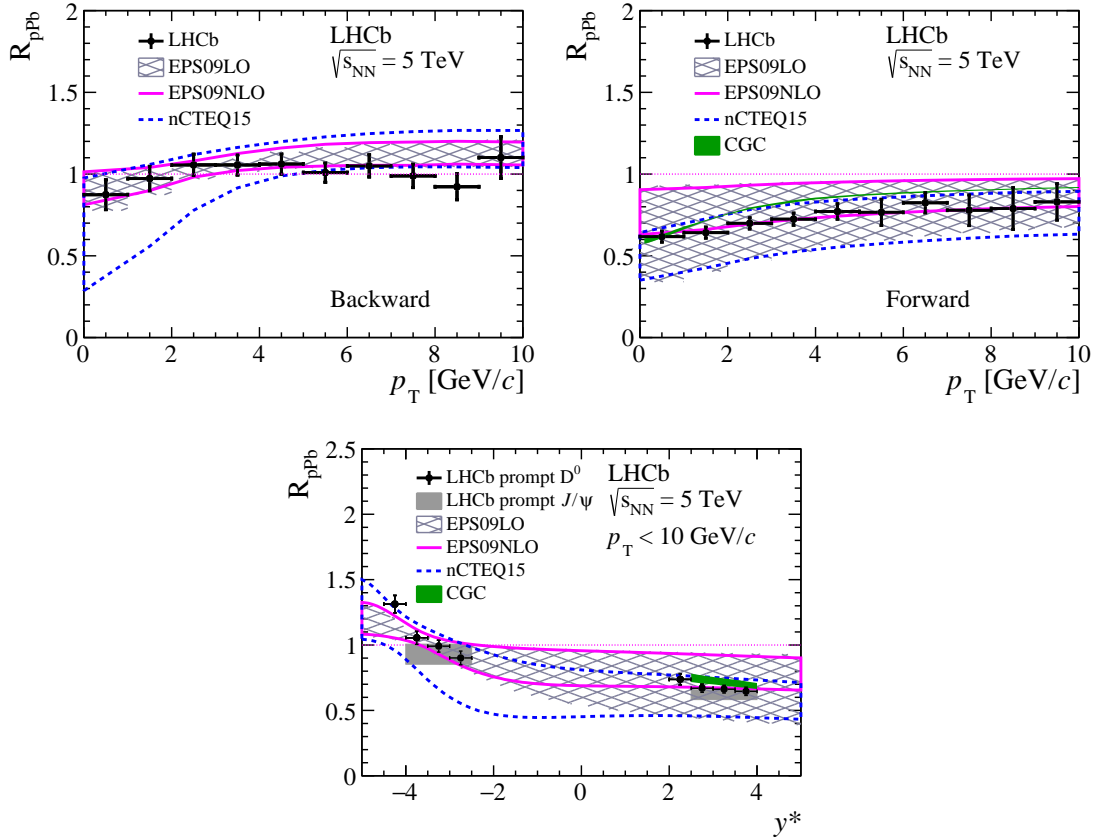


**Figure 3:** Prompt  $D^0$   $R_{pPb}$  for top left:  $Pb p$  as a function of  $p_T$ , top right:  $pPb$  as a function of  $p_T$  and bottom: as a function  $y^*$ .

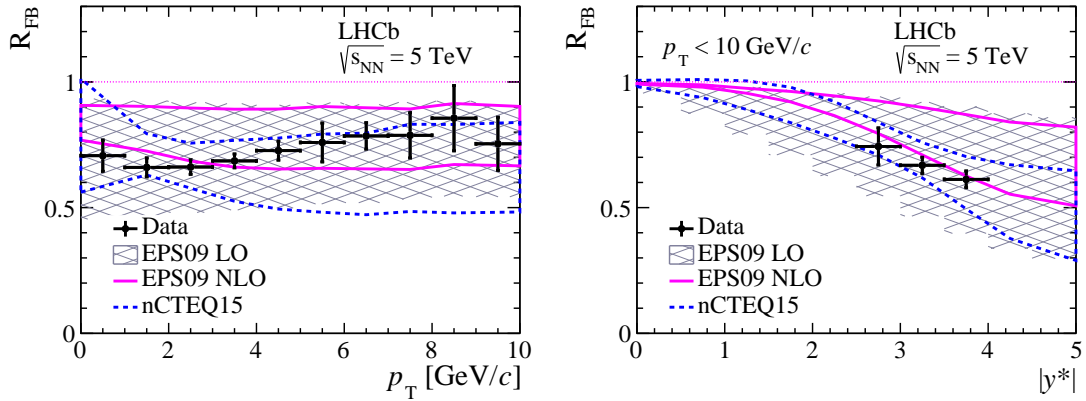


**Figure 4:** Prompt  $D^0$   $R_{FB}$  as a function of left:  $p_T$  and right:  $y^*$ .

the data sample collected in 2016 in proton-lead collisions at 8.16 TeV: Figure 5 shows as example the signals obtained in the reconstruction of  $B_s^0$  and  $\Lambda_b^0$  decays. The study of their production will

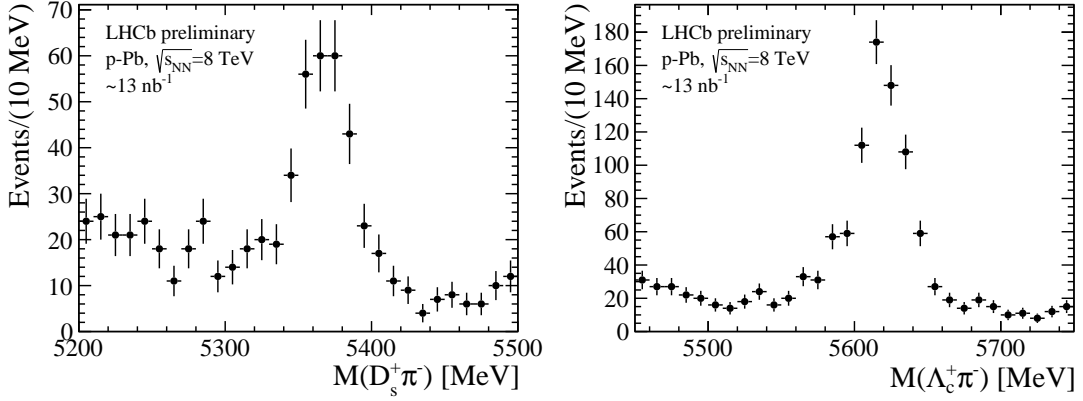


**Figure 5:** Left:  $B_s^0 \rightarrow D_s^- \pi^+$  and right:  $\Lambda_b^0 \rightarrow \Lambda_c^+ \pi^-$  invariant mass distributions in pPb collisions at 8.16 TeV.

give additional important information about the properties of the medium formed in heavy ion collisions.

## References

- [1] A. Andronic *et al.*, Eur. Phys. J. C **76** (2016) 107, arXiv:1506.03981 [nucl-ex].
- [2] NA50 collaboration, M. C. Abreu *et al.*, Phys. Lett. B **410** (1997) 327.
- [3] PHENIX collaboration, A. Adare *et al.*, Phys. Rev. Lett. **98** (2007) 232301, nucl-ex/0611020.
- [4] ALICE collaboration, B. Abelev *et al.*, Phys. Rev. Lett. **109** (2012) 072301, arXiv:1202.1383 [hep-ex].
- [5] CMS collaboration, V. Khachatryan *et al.*, Eur. Phys. J. C **77** (2017) 252, arXiv:1610.00613 [nucl-ex].
- [6] LHCb collaboration, R. Aaij *et al.*, arXiv:1707.02750 [hep-ex].
- [7] LHCb collaboration, A. A. Alves Jr *et al.*, “The LHCb detector at the LHC”, JINST **3** (2008) S08005.
- [8] LHCb Collaboration, R. Aaij *et al.*, Int. J. Mod. Phys. A **30** (2015) 1530022, arXiv:1412.6352 [hep-ex].
- [9] E. Maurice for the LHCb collaboration, arXiv:1708.05184 [hep-ex].
- [10] G. Graziani for the LHCb Collaboration, arXiv:1705.05438 [hep-ex].
- [11] LHCb collaboration, R. Aaij *et al.*, JINST **7** (2012) P01010, arXiv:1110.2866 [hep-ex].
- [12] J. P. Lansberg and H. S. Shao, Eur. Phys. J. C **77** (2017) 1, arXiv:1610.05382 [hep-ph].
- [13] K. J. Eskola, H. Paukkunen and C. A. Salgado, JHEP **0904** (2009) 065, arXiv:0902.4154 [hep-ph].
- [14] K. Kovarik *et al.*, Phys. Rev. D **93** (2016) 085037, arXiv:1509.00792 [hep-ph].
- [15] LHCb collaboration, R. Aaij *et al.*, JHEP **1706** (2017) 147, arXiv:1610.02230 [hep-ex].
- [16] B. Ducloué, T. Lappi and H. Mäntysaari, Phys. Rev. D **91** (2015) 114005, arXiv:1503.02789 [hep-ph].